A Mechanism for the Effect of Tropospheric Jet Structure on the Annular Mode–Like Response to Stratospheric Forcing

ISLA R. SIMPSON

Department of Physics, University of Toronto, Toronto, Ontario, Canada

MICHAEL BLACKBURN

National Centre for Atmospheric Science, University of Reading, Reading, United Kingdom

JOANNA D. HAIGH

Department of Physics, Imperial College London, London, United Kingdom

(Manuscript received 13 July 2011, in final form 29 January 2012)

ABSTRACT

For many climate forcings the dominant response of the extratropical circulation is a latitudinal shift of the tropospheric midlatitude jets. The magnitude of this response appears to depend on climatological jet latitude in general circulation models (GCMs): lower-latitude jets exhibit a larger shift.

The reason for this latitude dependence is investigated for a particular forcing, heating of the equatorial stratosphere, which shifts the jet poleward. Spinup ensembles with a simplified GCM are used to examine the evolution of the response for five different jet structures. These differ in the latitude of the eddy-driven jet but have similar subtropical zonal winds. It is found that lower-latitude jets exhibit a larger response due to stronger tropospheric eddy–mean flow feedbacks.

A dominant feedback responsible for enhancing the poleward shift is an enhanced equatorward refraction of the eddies, resulting in an increased momentum flux, poleward of the low-latitude critical line. The sensitivity of feedback strength to jet structure is associated with differences in the coherence of this behavior across the spectrum of eddy phase speeds. In the configurations used, the higher-latitude jets have a wider range of critical latitude locations. This reduces the coherence of the momentum flux anomalies associated with different phase speeds, with low phase speeds opposing the effect of high phase speeds. This suggests that, for a given subtropical zonal wind strength, the latitude of the eddy-driven jet affects the feedback through its influence on the width of the region of westerly winds and the range of critical latitudes on the equatorward flank of the jet.

1. Introduction

The annular modes, which represent migrations in latitude of the tropospheric midlatitude jets, are the dominant modes of variability in tropospheric zonal mean zonal wind in both the Northern and Southern Hemispheres (e.g., Thompson and Wallace 2000; Lorenz and Hartmann 2001, 2003; Kushner 2010). The response to many different climate forcings also projects strongly onto the annular modes—for instance, increased anthropogenic emissions of greenhouse gases (Fyfe and Saenko 2006; Miller et al. 2006), ozone depletion (Thompson and Solomon 2002), El Niño (Seager et al. 2003), and solar variability (Haigh et al. 2005, hereafter HBD05). Thus, understanding annular mode–like responses is relevant for understanding many different aspects of climate variability and change.

Although many modeling studies agree on the qualitative sense of the response to each of these forcings, it has recently become apparent that the response magnitude is model dependent. Son et al. (2010) analyzed the poleward shift of the Southern Hemisphere (SH) jet in response to ozone depletion in the Chemistry–Climate Model Validation (CCMVal2) models (SPARC CCMVal 2010). They found considerable variability in the magnitude

Corresponding author address: Isla Simpson, Department of Physics, University of Toronto, 60 St George St., Toronto, ON M5S 1A7, Canada.
E-mail: isla@atmosp.physics.utoronto.ca

DOI: 10.1175/JAS-D-11-0188.1

of the zonal wind response, with a near-linear relationship between this and the climatological jet latitude. Kidston and Gerber (2010) found a similar relationship for the response to increased greenhouse gases. They compared the magnitude of the poleward shift of the SH jet between the Coupled Model Intercomparison Project (phase 3; CMIP3) models. Again, a near-linear relationship between the magnitude of the shift and the climatological jet latitude was found. The latitude dependence of the response to a forcing occurs together with a latitude dependence of the time scale of natural variability (Kidston and Gerber 2010), consistent with the fluctuation–dissipation theorem (FDT) (Leith 1975). This joint dependence suggests that, when the midlatitude jet exists at a lower latitude, the feedbacks between the eddies and the mean flow are stronger.

The SH midlatitude jet in climate models is generally biased toward low latitudes relative to observations (Fyfe and Saenko 2006). Thus, if jet latitude is a major factor affecting the magnitude of the predicted shift of the jet in response to a forcing, then models are likely to be consistently predicting too large a shift in the SH. Changes in the zonal mean circulation can impact other aspects of the climate system, such as the uptake of carbon dioxide by the Southern Ocean (Zickfeld et al. 2007; Lenton et al. 2009; Swart and Fyfe 2011) or sea ice extent (Sigmond and Fyfe 2010). Thus, biases in the predicted zonal mean circulation response may significantly alter model predictions of both regional-scale and global climate. It is therefore important to understand the factors that control the climatological location and variability of the midlatitude jet and to understand why the response to a forcing and the time scale of variability depends on jet structure.

Recently, a great deal of understanding has been obtained through the use of simplified general circulation models (sGCMs). The advantage of such models is that they are highly computationally efficient, allowing long simulations or large ensembles to be performed to investigate dynamical mechanisms. It has been shown that the decorrelation time scale of annular mode variability in sGCMs also depends on the jet latitude (Gerber and Vallis 2007; Gerber et al. 2008; Son and Lee 2005; Chan and Plumb 2009; Barnes et al. 2010; Simpson et al. 2010, hereafter SBHS10). In some cases it is found that simplified GCMs exhibit a bimodality in their jet latitude such that when the jet exists at a certain location, the variability is characterized by long time scale transitions between two preferred jet latitudes (Chan and Plumb 2009). In other cases, a monotonic relationship between jet latitude and decorrelation time scale is found (SBHS10). In the sGCM study of SBHS10 it was found that, for the case of heating of the equatorial stratosphere (which shifts the jet poleward), the magnitude of the poleward shift depended on the latitude of the climatological jet, with lower-latitude jets having a larger response to forcing than higher-latitude jets. The annular mode time scale was also longer for lower-latitude jets, consistent with the FDT.

The reason for this joint dependence of both the time scale of variability and the magnitude of response to a forcing on the climatological jet latitude in both comprehensive and simplified GCMs remains uncertain. Several hypotheses have been proposed. One argument is that the lower-latitude jets are simply able to move farther poleward before reaching some high-latitude limit (Kidston and Gerber 2010), although what sets this high-latitude limit is unclear. Another argument identifies a difference in the strength of the feedback between the eddies and the mean flow. Lee et al. (2007) and Son et al. (2008b) suggest that the dependence of the time scale of the natural variability on jet latitude in their sGCM simulations is related to the presence or absence of a low-latitude reflecting surface. The behavior of the natural variability of the different jet structures in SBHS10, however, was found to be inconsistent with this.[1] Another possibility, proposed by Barnes et al. (2010), is that, for lower-latitude jets, the presence of poleward wave breaking narrows the region of eddy momentum flux convergence, resulting in a stronger feedback, whereas higher-latitude jets exhibit a reflecting surface on the poleward side of the jet, no poleward wave breaking, and a weaker eddy feedback. This is unlikely to be able to explain the dependence in the forced runs of SBHS10, where poleward breaking waves do not appear to play a role in the response or in the difference in response magnitudes between different jets and none of the jet structures exhibits a reflecting surface on the poleward side of the jet (in Fig. 10 of SBHS10, the refractive index increases to a maximum on the poleward side of the jet, indicating the presence of a critical latitude).

The present study follows that of SBHS10 and addresses the question of why the magnitude of the zonal wind response depends on jet latitude for a particular forcing case, heating of the equatorial stratosphere. The original motivation for this forcing was to represent the heating of the equatorial lower stratosphere associated with solar variability. The mechanism involved in

[1] SBHS10 incorrectly stated that a subtropical reflecting surface is present for the most poleward jet (TR5). In fact a critical line ($u = c = 8$ m s^{-1}) is found before $\overline{q}_y = 0$ equatorward of the jet in all five cases.

producing the tropospheric response to this forcing has already been investigated in detail (HBD05; Simpson et al. 2009, hereafter SBH09), so it is used here to investigate the latitude dependence. While this forcing is different from climate change or ozone depletion, it acts to shift the jet poleward in a similar manner. It will be shown that the dependence of the magnitude of response on jet latitude is related to the strength of the feedback between the eddies and the tropospheric zonal wind anomalies and therefore could be relevant for any forcing that acts to shift the jet.

The model, experiments, and diagnostics are described in section 2. A summary of the experiments and the results of HBD05, SBH09, and SBHS10 is given in section 3. The time evolution in response to stratospheric heating for five different jet structures is examined in section 4. Section 5 proposes a mechanism for the difference in eddy feedback strength between the jets, and conclusions will be drawn in section 6.

2. The model, experiments, and cospectrum analysis

a. The model

The sGCM used in the following study is the same as that used in HBD05, SBH09, and SBHS10. It is a spectral dynamical core as described by Hoskins and Simmons (1975) with the modification to include the angular momentum conserving vertical discretization of Simmons and Burridge (1981) while retaining the original sigma coordinate. Triangular truncation at wavenumber 42 is used and there are 15 levels between the surface and $\sigma = 0.0185$. Unlike some sGCMs used to investigate stratosphere–troposphere coupling, the model intentionally does not include a fully resolved stratosphere and does not exhibit a stratospheric polar vortex.

The mean state is maintained by Newtonian relaxation of temperature toward a zonally symmetric equilibrium state. In the original configuration used in HBD05 and SBH09, this relaxation temperature distribution is based on that described by Held and Suarez (1994) and given by

$$T_{\mathrm{ref}}(\phi, p) = \max\left\{(T_{\mathrm{tpeq}} - \Delta T_{\mathrm{tp}} \sin^2\phi),\ \left[T_o - \Delta T_y \sin^2\phi - (\Delta\theta_{\mathrm{eq}} \cos^2\phi + \Delta\theta_{\mathrm{pl}} \sin^2\phi) \log\left(\frac{p}{p_o}\right)\right]\left(\frac{p}{p_o}\right)^{\kappa}\right\}, \quad (1)$$

where p_o is the reference surface pressure (=1000 hPa), T_{tpeq} is the equatorial tropopause temperature, ΔT_{tp} is the difference in temperature between the equatorial and polar tropopause, T_o is the surface temperature at the equator, ΔT_y is the difference between the equatorial and polar surface temperature, and $\Delta\theta_{\mathrm{eq}}$ and $\Delta\theta_{\mathrm{pl}}$ are the increase in potential temperature with an increase in altitude of one pressure scale height at the equator and poles, respectively. In the original Held–Suarez configuration these parameters are set to $T_{\mathrm{tpeq}} = 200$ K, $\Delta T_{\mathrm{tp}} = 0$ K, $T_o = 315$ K, $\Delta T_y = 60$ K, $\Delta\theta_{\mathrm{eq}} = 10$ K, and $\Delta\theta_{\mathrm{pl}} = 0$ K. This relaxation temperature profile can be seen in Fig. 1c. The temperature is relaxed toward this profile on a time scale of 40 days for $\sigma < 0.7$ (representing radiation and deep moist processes), reducing to 4 days at the equatorial surface (representing the planetary boundary layer). Boundary layer friction is represented by Rayleigh damping of winds below $\sigma = 0.7$ with a time scale of 1 day at the surface. The upper boundary condition is reflective (i.e., $\partial\sigma/\partial t = 0$ at the model lid). There is no topography or other large-scale zonally asymmetric forcing, so planetary waves are weak and are generated only by upscale energy transfer from the dominant synoptic scales. Baroclinic eddies dominate the wave spectrum with peak amplitude at zonal wavenumbers 5–7. These are initiated through a white noise perturbation applied to the surface pressure at the beginning of each equilibrium integration.

b. The experiments

An advantage of using sGCMs in this Newtonian forced configuration is that the climatological jet structures can easily be altered and perturbations can easily be applied by altering the temperature profile toward which the model is relaxed. The model experiments that will be examined in the following are the same as those in SBHS10 but for completeness they will be described again here.

The response to heating of the equatorial stratosphere in the model will be examined (the E5 heating case of HBD05 and SBH09, the letter E referring to equatorial and 5 referring to the maximum heating of 5 K at the equator). This heating perturbation is applied by changing the parameters T_{tpeq} and ΔT_{tp} to 205 and 5 K, respectively (see shading in Fig. 1c). It will be applied to five different tropospheric climatologies, produced by changing the tropospheric relaxation temperature profile. The original configuration, denoted TR3, uses the original Held–Suarez T_{ref} (Fig. 1c). To generate four new tropospheres (TR1, TR2, TR4 and TR5), this original configuration is altered by adding the perturbations shown in

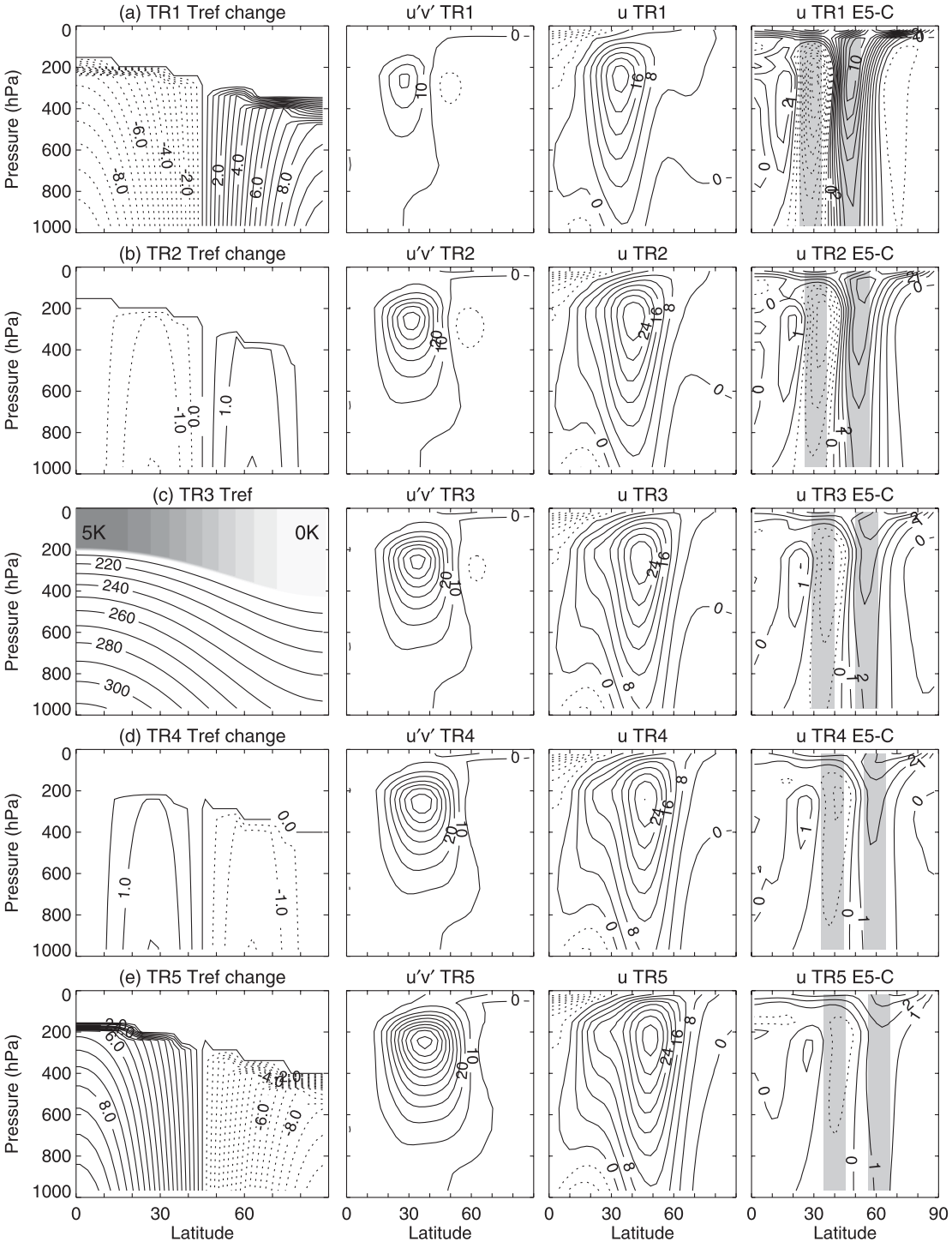

FIG. 1. (column1) (c) The Held–Suarez relaxation temperature profile (TR3) (contours) together with the temperature perturbation that is applied to the stratosphere for the E5 heating case (shading, shading interval = 0.5 K). (a),(b),(d),(e) The temperature perturbation added to (c) to create the four troposphere TR1, TR2, TR4, and TR5, respectively (contour interval = 0.5 K). (column 2) Control run horizontal eddy momentum flux for each troposphere (contour interval = 10 $m^2 s^{-2}$). (column 3) Control run zonal wind for each troposphere (contour interval = 4 m s^{-1}). (column 4) Equilibrium anomaly in zonal wind in response to E5 heating for each troposphere (contour interval = 1 m s^{-1}). Solid and dotted contours represent positive and negative values, respectively. All panels with the exception of column 2 are reproduced from SBHS10. The gray regions in column 4 represent 10° latitude bands in the region of maximum zonal wind decrease and increase that are used later to quantify eddy feedbacks.

TABLE 1. Summary of the relaxation temperature profiles for the jet structures TR1–TR5.

Name	T_{ref} for the control simulation
TR1	Eq. (1), $T_o = 305$ K, $\Delta T_y = 40$ K
TR2	Eq. (2), $T_o = 315$ K, $\Delta T_y = 60$ K, $\overline{Q} = -2$ K
TR3	Eq. (1), $T_o = 315$ K, $\Delta T_y = 60$ K
TR4	Eq. (2), $T_o = 315$ K, $\Delta T_y = 60$ K, $\overline{Q} = 2$ K
TR5	Eq. (1), $T_o = 325$ K, $\Delta T_y = 80$ K

Figs. 1a, 1b, 1d, and 1e, and summarized in Table 1, onto the original T_{ref}.

Midlatitude baroclinicity increases from TR1 to TR5. TR1 reduces and TR5 enhances the equator to pole temperature difference by 20 K, by changing the parameters T_o and ΔT_y in Eq. (1) to 305 and 325 K and to 40 and 80 K, respectively. TR2 and TR4 have a different relaxation temperature profile given by

$$T_{\text{ref}}(\phi, p) = [\text{Eq. (1), rhs}] + \overline{Q}\cos[2(\phi - \pi/4)]\sin[4(\phi - \pi/4)]\left(\frac{p}{p_o}\right)^{\kappa}, \quad (2)$$

where $\overline{Q}$ is +2 K for TR4 and −2 K for TR2. Therefore, TR2 has a reduced midlatitude baroclinicity but with the maximum change in T_{ref} occurring in the subtropics and subpolar regions. These changes are reversed in TR4. The five different tropospheric T_{ref} distributions produce different strengths of eddy fluxes and result in different strengths and latitudes of the tropospheric jet, as can be seen in columns 2 and 3 of Fig. 1. The eddy momentum fluxes increase in strength from TR1 to TR5 and the midlatitude jet strengthens, moves poleward, and becomes increasingly separated from the subtropical jet. The responses to equatorial stratospheric heating shown in SBHS10 are reproduced in column 4 of Fig. 1 and will be discussed in the following section. These equilibrium responses are produced from the difference between a 50 000-day integration with E5 heating applied and a 50 000-day control run, for each of the five tropospheres.

The equilibrium response cannot be used to separate cause and effect due to the presence of strong eddy–mean flow feedbacks, so spinup ensemble experiments will be used to examine the time evolution of the response. In SBHS10, the time evolution of 200 member ensembles for tropospheres TR2 and TR4 was examined. Here, the number of ensemble members is increased to 1000 and all five tropospheres are examined. The 1000 ensemble members are started from 50-day intervals of the relevant control integration. Each ensemble member is run for 150 days with the E5 perturbation to T_{ref} continually applied. In the following, the anomalies over the spinup relative to the relevant control integration will be examined.

c. *The eddy flux cospectra diagnostic*

The circulation in midlatitudes is determined by strong coupling between the zonal mean state and the fluxes of heat and momentum due to transient synoptic-scale eddies. The cospectra of these eddy fluxes will be analyzed, following the method of Hayashi (1971). The eddy fluxes are calculated from daily instantaneous gridded data and are separated into contributions over wavenumber–phase speed (k, c) space at each latitude. Summing over the zonal wavenumber then allows the eddy fluxes to be examined as a function of latitude and phase speed. The refractive properties of the atmosphere, and thus the direction of eddy propagation, depend on phase speed (e.g., Matsuno 1970; Karoly and Hoskins 1982), so it is important to consider how different phase speeds behave. Randel and Held (1991) demonstrated that, consistent with linear theory, the momentum fluxes associated with tropospheric synoptic-scale eddies are restricted to the region between the low- and high-latitude critical lines (where the zonal mean zonal wind $\overline{u}$ equals the phase speed). Moreover, the maximum wave drag [or Eliassen–Palm (E-P) flux convergence] associated with the eddies occurs in a region just poleward of the low-latitude critical line, where the eddies break. Thus, the distribution of eddy fluxes, and the zonal mean circulation, depends crucially on the eddy phase speed. Here, the cospectra are analyzed as a function of angular phase speed ($c_A = c/\cos\phi$) which is conserved following waves propagating in the meridional direction (Randel and Held 1991). When relating momentum fluxes to critical lines it is therefore necessary to compare c_A with $\overline{u}/\cos\phi$.

3. An overview of the tropospheric response to equatorial stratospheric heating

The response to the E5 stratospheric heating and its mechanism have been discussed extensively in HBD05, SBH09, and SBHS10, so only an overview is given here. HBD05 found that the equilibrium response for the TR3 tropospheric climatology is a poleward shift of the tropospheric midlatitude jet. SBHS10 showed that the magnitude of the response depends on the climatological jet latitude for the TR1–TR5 climatologies.

The equilibrium responses, reproduced in column 4 of Fig. 1, comprise a dipole in the zonal mean zonal wind approximately centered on the jet. The dipole is the signature of a poleward jet shift, the magnitude of which is shown in Fig. 2a by the location of maximum zonal wind in the lower troposphere (675 hPa), so as to describe the

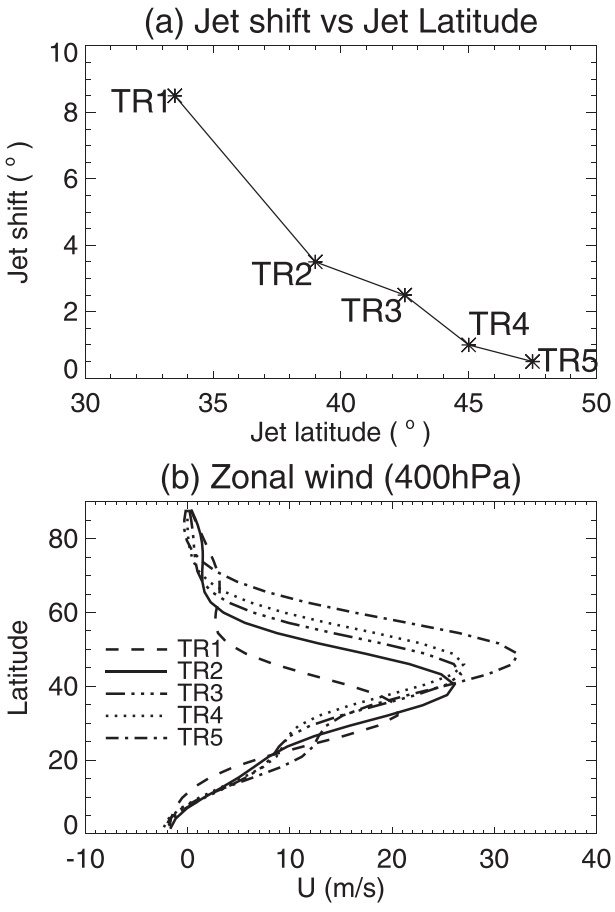

FIG. 2. (a) Change in jet latitude in response to E5 heating vs climatological jet latitude for each troposphere. Jet latitude is taken to be the maximum in zonal mean zonal wind at 675 hPa after first interpolating the zonal wind onto a 0.5° latitude grid using cubic splines. (b) Latitudinal structure of zonal mean zonal wind for each jet structure in the upper troposphere (at 400 hPa).

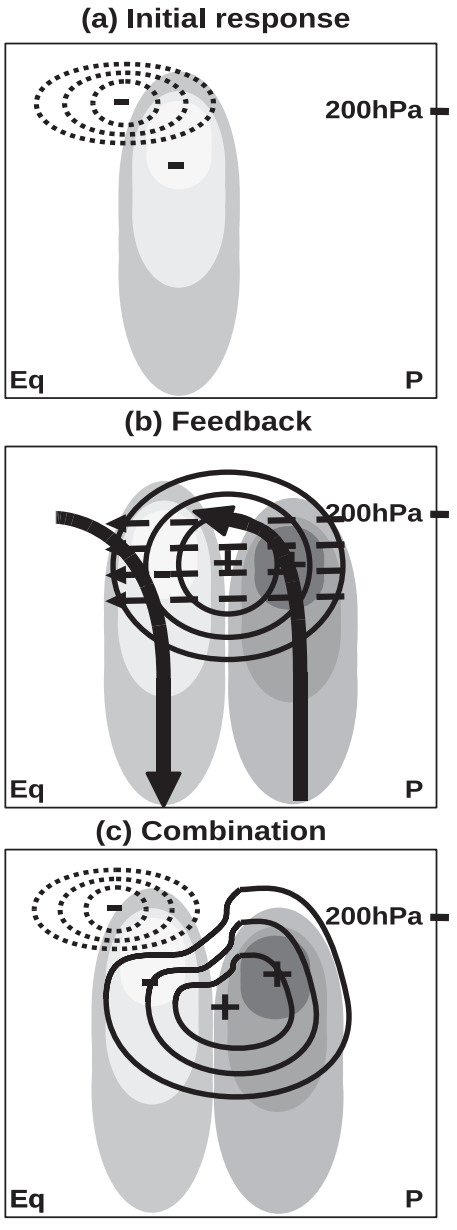

FIG. 3. Schematic of the proposed mechanism for a tropospheric response to heating of the equatorial stratosphere. (a) The initial response. The altered temperature gradient around the tropopause weakens the upward flux of wave activity and results in reduced $\overline{u'v'}$ around the tropopause (dotted contours). This drives a decrease in $\overline{u}$ on the equatorward side of the midlatitude jet (shading) and an acceleration farther equatorward (not shown). (b) The feedbacks that both enhance the reduction in $\overline{u}$ on the equatorward side of the jet and accelerate the zonal wind on the poleward side of the jet. The altered meridional wind shear refracts the wave activity equatorward (dashed arrows) and the shift in the zonal wind displaces the baroclinicity and eddy source latitude (solid arrows). Both feedbacks enhance the equatorward propagation of the eddies across the climatological jet center, increasing the poleward eddy momentum flux there, enhancing the zonal wind anomalies. (c) The combination of eddy momentum flux anomalies associated with the initial response and the feedback.

eddy-driven jet. The responses are all qualitatively similar but there is a monotonic relationship between climatological jet latitude and the magnitude of the response. The lower-latitude jets produce a stronger response, with almost an order of magnitude difference between TR1 and TR5.[2]

The mechanism behind the response has been discussed in detail by SBH09 for the TR3 climatology. Of particular relevance for understanding the latitude dependence of the response magnitude is the distinction between two components of the response: the initial response and the feedback. These are summarized in schematic form in Fig. 3. The initial response, depicted

[2] Note that none of these jet structures exhibits a bimodality in jet location, which has been found to give rise to large responses in other studies (Chan and Plumb 2009).

schematically in Fig. 3a, is associated with a lowering of the tropopause on the equatorward side of the jet, at the base of the stratospheric heating. This increases the static stability in that region, which alters the propagation of the synoptic-scale baroclinic eddies. In the climatology, eddy growth is centered on the latitude of the jet maximum. Wave activity propagates upward (associated with a poleward heat flux) and is refracted mainly equatorward (associated with a poleward momentum flux) consistent with the behavior of nonlinear baroclinic life cycles (e.g., Thorncroft et al. 1993). The increased static stability beneath the region of stratospheric warming reduces the upward and equatorward flux of wave activity. The result is that the wave activity converges slightly lower and closer to the latitude of the jet. This results in a decrease in poleward momentum flux around the tropopause, which directly decelerates the zonal wind on the equatorward side of the jet around the tropopause and, through the driving of an anomalous meridional circulation, results in a zonal wind deceleration lower down in the troposphere.

This initial response triggers a feedback, which consists of two components depicted schematically in Fig. 3b. In the first component, the initial zonal wind deceleration alters the meridional wind shear, which increases the equatorward refraction of eddies toward the region of reduced westerly wind. This occurs throughout the upper half of the troposphere. This increases poleward momentum flux across the jet center, which enhances the initial deceleration on the equatorward side of the jet and accelerates the zonal wind on the poleward side. These zonal wind accelerations further increase the meridional wind shear and equatorward propagation of the eddies, providing a positive feedback. In the second component of the feedback, the baroclinicity shifts with the jet, resulting in an anomalous source of eddy activity on the poleward side of the jet and a reduced source on the equatorward side. The momentum fluxes associated with these anomalies in eddy source provide a further feedback onto the zonal wind anomalies (Robinson 2000; Kidston et al. 2010).

The equilibrium response, depicted schematically in Fig. 3c, is a combination of the initial response, which decelerates the zonal wind on the equatorward side of the jet, and the feedbacks that enhance that deceleration and accelerate the zonal wind on the poleward side of the jet. Thus, the equilibrium eddy momentum flux anomalies are a combination of decreased momentum flux around the tropopause in the region of increased stratospheric temperature on the equatorward side of the jet and increased momentum flux across the jet center. Both of these anomalies result in an eddy momentum flux divergence on the equatorward side of the jet and the feedback processes also result in an eddy momentum flux convergence on the poleward side of the jet.

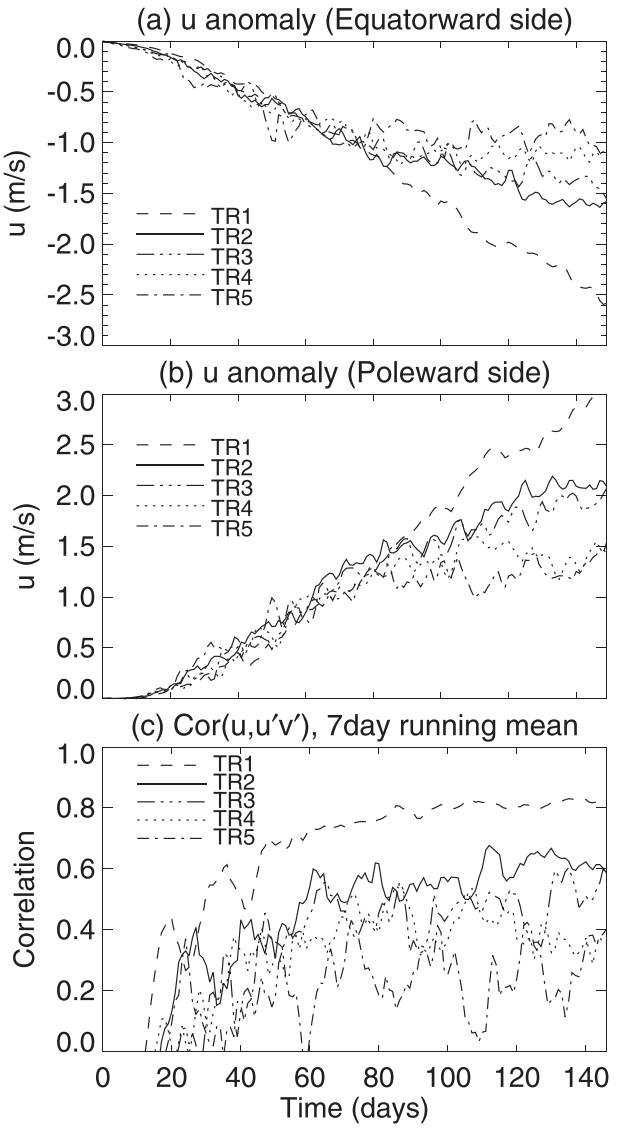

FIG. 4. Time evolution over the E5 spinups of (a) vertically averaged zonal wind anomaly on the equatorward side of the jet, (b) vertically averaged zonal wind anomaly on the poleward side of the jet, and (c) correlation between the spatial patterns of the zonal wind anomalies and the eddy momentum flux convergence between 300 hPa and the surface (7-day running mean). Anomalies in (a) and (b) are averaged over the gray shaded regions in Fig. 1.

The questions addressed here are: 1) which of the above processes leads to the sensitivity of the response to the climatological jet latitude? and 2) how does this effect take place?

4. The spinup evolution

a. Evolution of the response

Figures 4a and 4b show the time evolution of the vertically averaged zonal wind anomalies on the equatorward

and poleward side of the jet. These are averaged over the gray shaded regions in column 4 of Fig. 1. The data were first interpolated onto a 0.5° latitude grid using cubic splines. The locations of the maximum and minimum zonal wind anomalies at 675 hPa at equilibrium were obtained and the data were then averaged over the 10° latitude band surrounding those locations. The difference in zonal wind evolution of each of the tropospheres becomes clear after about day 80: the zonal wind anomalies level off and reach equilibrium much sooner for the higher-latitude jets, while the anomalies for the lower-latitude jets continue to grow.

Figure 4c provides a measure of the effectiveness of the eddy momentum flux feedback onto the zonal flow anomalies in the troposphere. It shows the spatial correlation between the ensemble mean eddy momentum flux convergence and the zonal wind anomaly over all latitudes and pressures below 300 hPa after weighting each field by $\sqrt{\cos\phi}$ to account for the decrease in area toward the pole. The correlation is smoothed with a 7-day running mean. The lower the latitude of the eddy-driven jet, the higher the correlation between the spatial patterns of zonal wind and eddy momentum flux convergence in the troposphere. This suggests a stronger tropospheric feedback for the lower-latitude jets. The correlation for the higher-latitude jets is not only smaller in magnitude but also more variable in time.

To confirm the role of this difference in eddy feedback in giving rise to the variation in response between the different jet structures, the time-integrated momentum equation will be examined. The Eulerian mean momentum equation can be written

$$\frac{\partial \overline{u}}{\partial t} = f\overline{v} - \frac{1}{a\cos^2\phi}\frac{\partial(\overline{u'v'}\cos^2\phi)}{\partial\phi} - k\overline{u} + \mathrm{AG}, \quad (3)$$

where overlined and primed quantities represent the zonal mean and the deviation from the zonal mean, respectively; u and v are the zonal and meridional wind components; a is the radius of the earth; k is the boundary layer frictional damping coefficient; and AG represents the ageostrophic terms. Since the time evolution of spinup anomalies is being investigated here, the anomaly of each term relative to the relevant control simulation will be considered.

Equation (3) can be solved for $\overline{u}$, as in SBH09, to give

$$\overline{u}(t) - \overline{u}(0) = \frac{1}{e^{kt}}\left[\int_0^t e^{kt'} f\overline{v}\, dt' + \int_0^t -e^{kt'}\frac{1}{a\cos^2\phi}\frac{\partial(\overline{u'v'}\cos^2\phi)}{\partial\phi}\, dt' + \int_0^t e^{kt'}\mathrm{AG}\, dt'\right]. \quad (4)$$

The e^{kt} factors arise from the dependence of the frictional damping on $\overline{u}$ itself. This time-integrated equation has the advantage that the evolution of the zonal wind anomaly is much less noisy than the instantaneous acceleration. The relatively smooth evolution of the zonal wind can then be attributed to the three different terms: the Coriolis force acting on the meridional wind, the momentum flux convergence, and the ageostrophic terms, each taking account of the frictional damping below 700 hPa. Above this $k = 0$ and the exponential terms vanish. Thus, the vertical integral of the time-integrated Coriolis term does not vanish. Its low-level contribution is reduced by the frictional factor, so the integral takes the sign of the upper-tropospheric contribution.

To illustrate this zonal wind budget, the vertical average (from the model lid to the surface) of each of the terms for TR3 is shown in Fig. 5a, for the gray region on the equatorward side of the jet in Fig. 1, column 4. The actual zonal wind anomaly and the sum of the terms cannot be distinguished, demonstrating the accuracy of this method. In the vertical average, the easterly zonal wind anomaly is driven by momentum flux divergence and damped by the $f\overline{v}$ term, and the much smaller ageostrophic terms. Damping by the Coriolis term occurs in the upper troposphere, where $k = 0$. The meridional circulation effectively transfers momentum to the lower troposphere, where the Coriolis term is of opposite sign but its effect is reduced by friction.

Having established this diagnostic for quantifying contributions to the zonal wind anomalies, the momentum flux convergence term and the damping terms on the right-hand side of Eq. (4) are shown in Figs. 5b and 5c on the equatorward side of each of the jets. The $f\overline{v}$ and AG terms have been combined in Fig. 5c as their relative contributions differ slightly between the tropospheres, although not in a monotonic manner between TR1 and TR5. Figures 5b and c highlight an important aspect of the time evolution of the response. Initially the momentum flux convergence term and the opposing damping terms are larger for the higher-latitude jets but then subsequently increase more rapidly for the lower-latitude jets. These are time-integrated quantities, so when the evolution in Figs. 5b and 5c becomes approximately linear, the momentum forcing term in Eq. (3) no longer increases with time. Thus, for the higher-latitude jets, the (negative) eddy momentum flux convergence is initially larger but then ceases to increase. In contrast, the lower-latitude jets

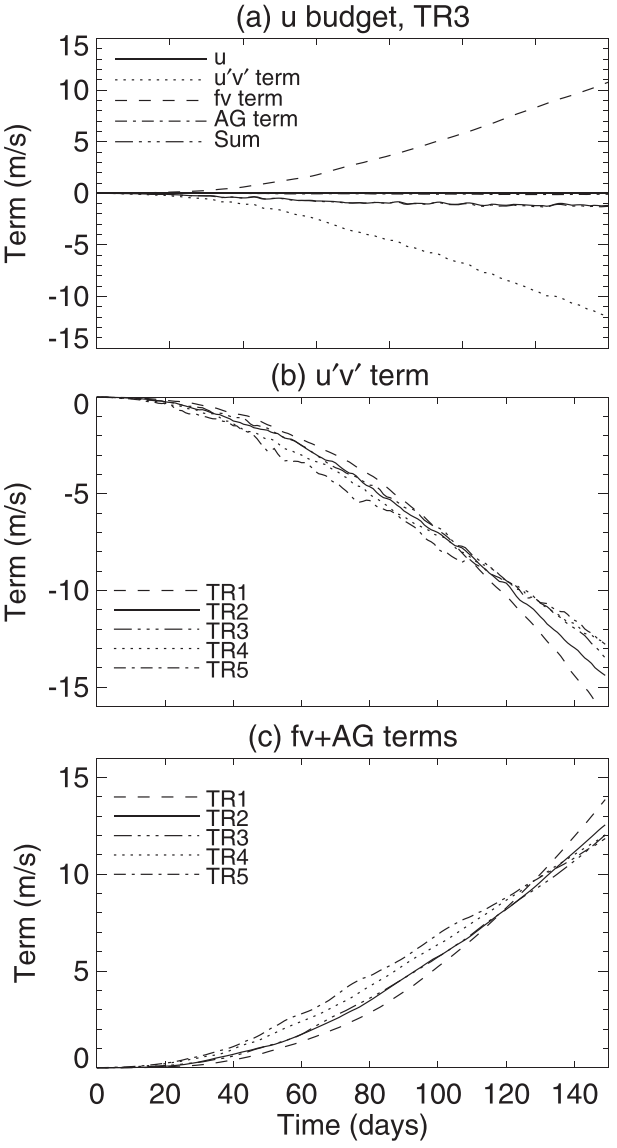

FIG. 5. (a) Time evolution of each of the terms in Eq. (4) for TR3, vertically averaged from the model lid to the surface. (b) Time evolution of the contribution to the vertically averaged zonal wind anomalies from the eddy momentum flux convergence for each jet. (c) As in (b), but for the $f\overline{v}$ and AG terms combined. All panels show the average over the shaded region on the equatorward side of the jets in Fig. 1.

have an initially smaller momentum flux convergence anomaly but it continues to increase with time.

b. *The initial response and feedbacks*

As discussed in section 3, there are two components of the overall response, an initial response to the stratospheric heating and the eddy feedbacks. One way in which the evolution of the terms in Fig. 5 could be obtained is if the initial response is larger for the higher-latitude jets but the eddy feedback is weaker. This can be verified by a more detailed examination of the spatial patterns of the eddy momentum flux response during two stages of the spinup: days 0–20, to examine the initial response, and days 40–70, to examine the feedback stage.

The eddy momentum flux anomalies $\overline{u'v'}$ averaged over days 0–20 are shown for each troposphere in the top row of Fig. 6. Over the first 20 days, the eddy momentum flux feedback has not yet become important. Only the initial response, which consists of a decrease in $\overline{u'v'}$ around the tropopause on the equatorward side of the jet, is apparent (compare with the schematic depiction in Fig. 3a). The initial direct response in temperature above the tropopause is very similar for each of the jets (not shown; see SBH09 for the TR3 anomalies), but the momentum flux response differs. Comparison of Fig. 6, row 1, with Fig. 1, column 2, shows that the larger response in momentum flux occurs for the tropospheres with greater climatological eddy fluxes (i.e., the response increases in magnitude from TR1 to TR5). This suggests that, for a given change in tropopause structure, the change in eddy fluxes is proportional to the climatological eddy fluxes.

The result is that the anomaly in $\overline{u'v'}$ divergence (Fig. 6, row 2) on the equatorward side of the jet increases from TR1 to TR5, decelerating the higher-latitude jets more strongly. This can be seen in row 3 of Fig. 6, which shows the zonal wind anomaly averaged over days 0–20. The higher-latitude jets, which have stronger climatological eddy fluxes, therefore have a stronger initial response.

Figure 7 shows the same data as Fig. 6, but for the average of days 40–70. This is a time when the feedback response has become important as can be seen by the $\overline{u'v'}$ anomaly plot in row 1, which can be compared with the schematic depictions in Fig. 3. The initial response, consisting of a decrease in $\overline{u'v'}$ around the tropopause and a corresponding flux divergence on the equatorward side of the jet (row 2), remains stronger for the higher-latitude jets and has grown in magnitude since the first 20 days. In addition, there is an increased $\overline{u'v'}$ across the jet center, which is associated with the feedback stage (compare with Fig. 3c). In the troposphere, this positive $\overline{u'v'}$ anomaly results in a flux divergence on the equatorward side of the jet and a flux convergence on the poleward side (Fig. 7, row 2), acting to feed back onto the zonal wind decrease on the equatorward side and accelerate the zonal wind on the poleward side. Note that the momentum flux anomaly associated with the feedback extends up to 50 hPa so that, above about 300 hPa, the anomalies consist of a combination of the initial response and the feedback.

There is a difference in the magnitude of the eddy momentum flux divergence on the equatorward side of the jet below 300 hPa between the different tropospheres. The increased divergence in the mid- to upper

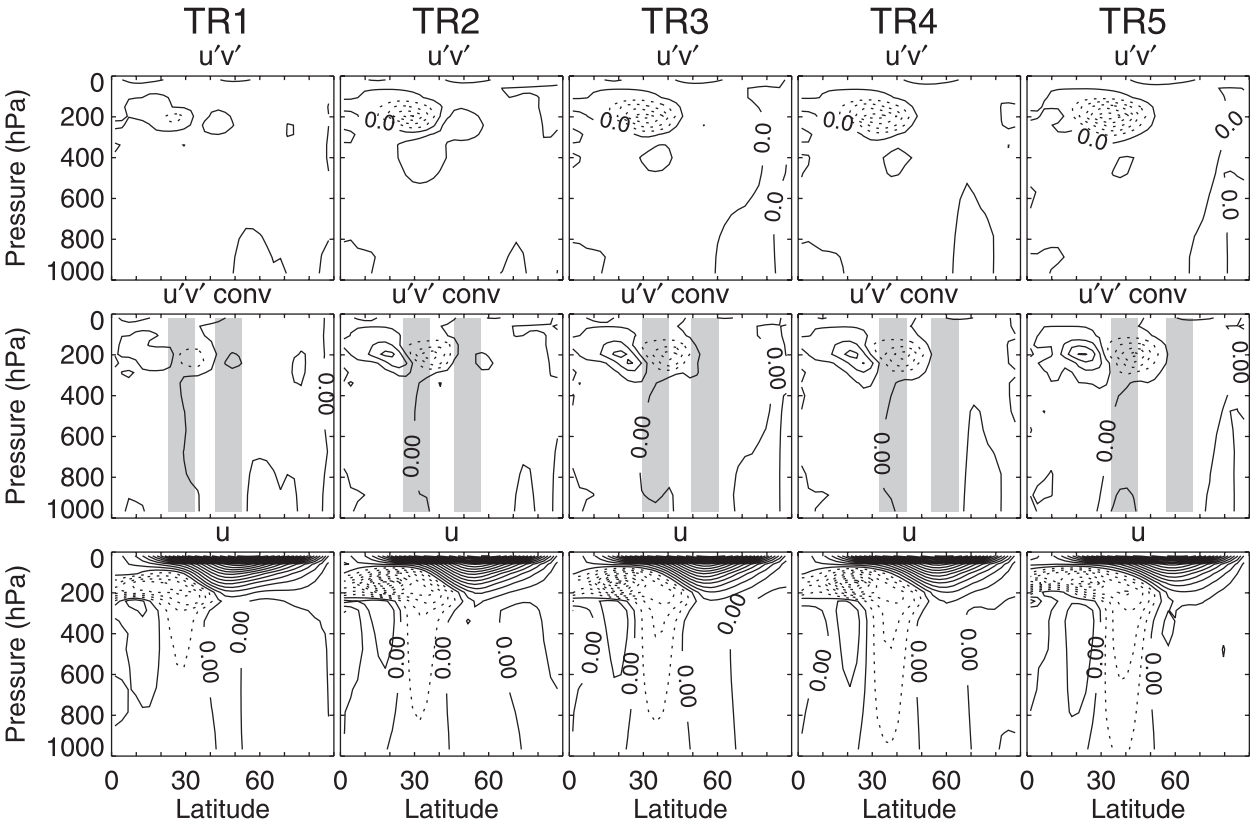

FIG. 6. Averages over days 0–20 of anomalies in (row 1) horizontal eddy momentum flux (contour interval = 0.5 $m^2\ s^{-2}$), (row 2) horizontal eddy momentum flux convergence (contour interval = 0.05 $m\ s^{-1}\ day^{-1}$), and (row 3) zonal mean zonal wind (contour interval = 0.05 $m\ s^{-1}$). (left to right) Tropospheres TR1–TR5 are shown. The 10° latitude bands on the equatorward and poleward side of the jet are shaded in gray for comparison in row 2.

troposphere is stronger for the lower-latitude jets (cf. the one negative contour in TR5 with the three negative contours in TR1 at around 400 hPa in Fig. 7, row 2). This is associated with a stronger and more meridionally confined $\overline{u'v'}$ anomaly in the troposphere for the lower-latitude jets (Fig. 7, row 1). This implies that the tropospheric eddy momentum flux feedback onto the zonal wind decrease on the equatorward side of the jet is stronger for the lower-latitude jets. It is possible that this difference in the strength of the eddy feedback could account for the difference in evolution over the spinup.

A crude method to separate the initial response, occurring above 300 hPa, from the eddy feedbacks, is to divide the time evolution of the vertically averaged eddy momentum flux term in the zonal wind budget [Eq. (4); Fig. 5b] into the contributions from the region between 0 and 300 hPa and the region between 300 hPa and the surface. While this does not completely separate the initial response from the feedbacks, since the feedbacks extend above 300 hPa, it will be shown that it is sufficient to identify the difference in feedback strength as being the dominant factor that gives rise to the different equilibrium responses of the jets. For the equatorward side of the jet, the full vertical average of the term is repeated in Fig. 8a for comparison. To recap, this time integration of the eddy momentum flux convergence term in Eq. (3) demonstrates that the anomaly is initially larger for the higher-latitude jets but it then ceases to increase. In contrast, the anomaly is initially smaller for the lower-latitude jets but it continues to increase with time. The reason for this behavior is investigated next.

In Fig. 8b it can be seen that the contribution of the eddy momentum flux convergence to the zonal wind anomalies on the equatorward side of the jet above 300 hPa is larger for the higher-latitude jets for the entire spinup evolution (i.e., the wrong sense to explain the difference in final responses). The anomalies here are dominated by the initial response, consistent with the discussion in the previous section that the initial response is larger for the higher-latitude jets because the climatological eddy fluxes are stronger. In contrast, the contribution from the eddy momentum flux convergence below 300 hPa (Fig. 8c) is much larger for the lower-latitude jets. Thus the vertically integrated momentum

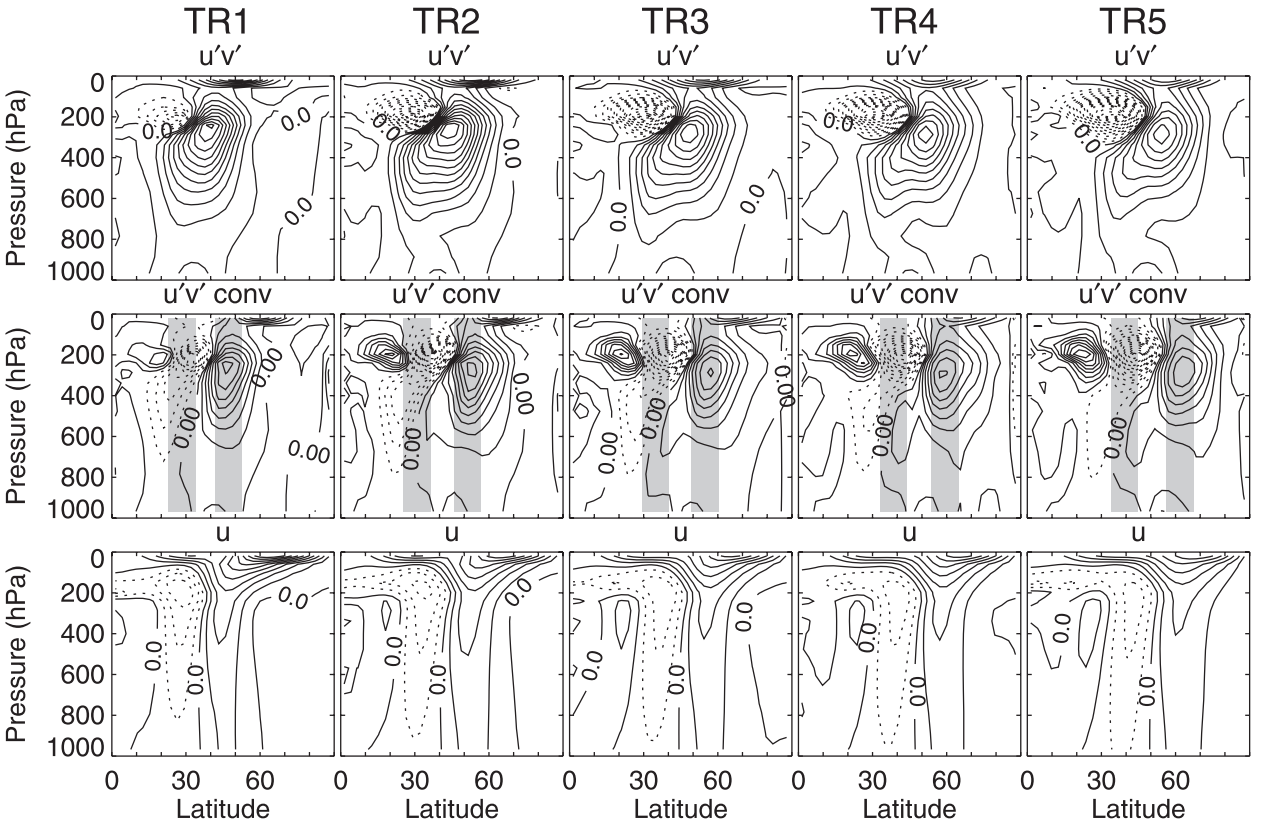

FIG. 7. As in Fig. 6, but for days 40–70. Contour intervals are $\overline{u'v'} = 0.5$ m^2 s^{-2}, $\overline{u'v'}$ convergence = 0.05 m s^{-1} day^{-1}, and $U = 0.5$ m s^{-1}.

flux convergence term in Fig. 8a begins to increase more rapidly for the lower-latitude jets from days 40 to 70 predominantly because of a difference that can be identified at these tropospheric levels (i.e., it is associated with the feedback).

This same decomposition on the poleward side of the jet reveals that the tropospheric contribution there only begins to differ between the tropospheres once the zonal winds begin to differ significantly, which is after about day 80 (Fig. 4b). This is unlike the term on the equatorward side of the jet in Figs. 8c and 7, row 2, which differs significantly between the tropospheres before day 80.

This zonal wind budget analysis reveals that the tropospheric responses begin to differ because of a difference in the strength of the eddy feedback on the equatorward side of the jet. It takes about 80 days before this difference in feedback strength manifests itself in the zonal wind. Prior to this the higher-latitude jets have a stronger initial response to the stratospheric heating that dominates over their weaker feedback, resulting in a larger zonal wind response in that initial period. In contrast, the lower-latitude jets have a weaker initial response but a stronger feedback. Once the stratospheric heating equilibrates, the initial response no longer increases, whereas the feedback response does, until eventually the zonal wind anomalies become sufficiently large that the surface friction balances the eddy momentum flux convergence anomalies. The situation brought about by this particular forcing and these particular jet structures is somewhat fortuitous, as it means that prior to about day 80 the zonal wind anomalies do not differ significantly between the tropospheres but the feedback strength does. This time period therefore provides an opportunity to understand why the eddy feedbacks differ, before the zonal wind anomalies themselves differ, which would itself induce a difference in feedback strength.

5. Why do lower-latitude jets have a stronger eddy feedback?

In Fig. 7 it can be seen that there is a difference in the strength of the eddy momentum flux feedback on the equatorward side of the jet stretching from about 300 to 600 hPa. One of the dominant feedbacks producing this momentum flux anomaly across the jet center is an increased equatorward refraction associated with the change in meridional wind shear. However, a difference in this refraction feedback is unlikely to be able to explain

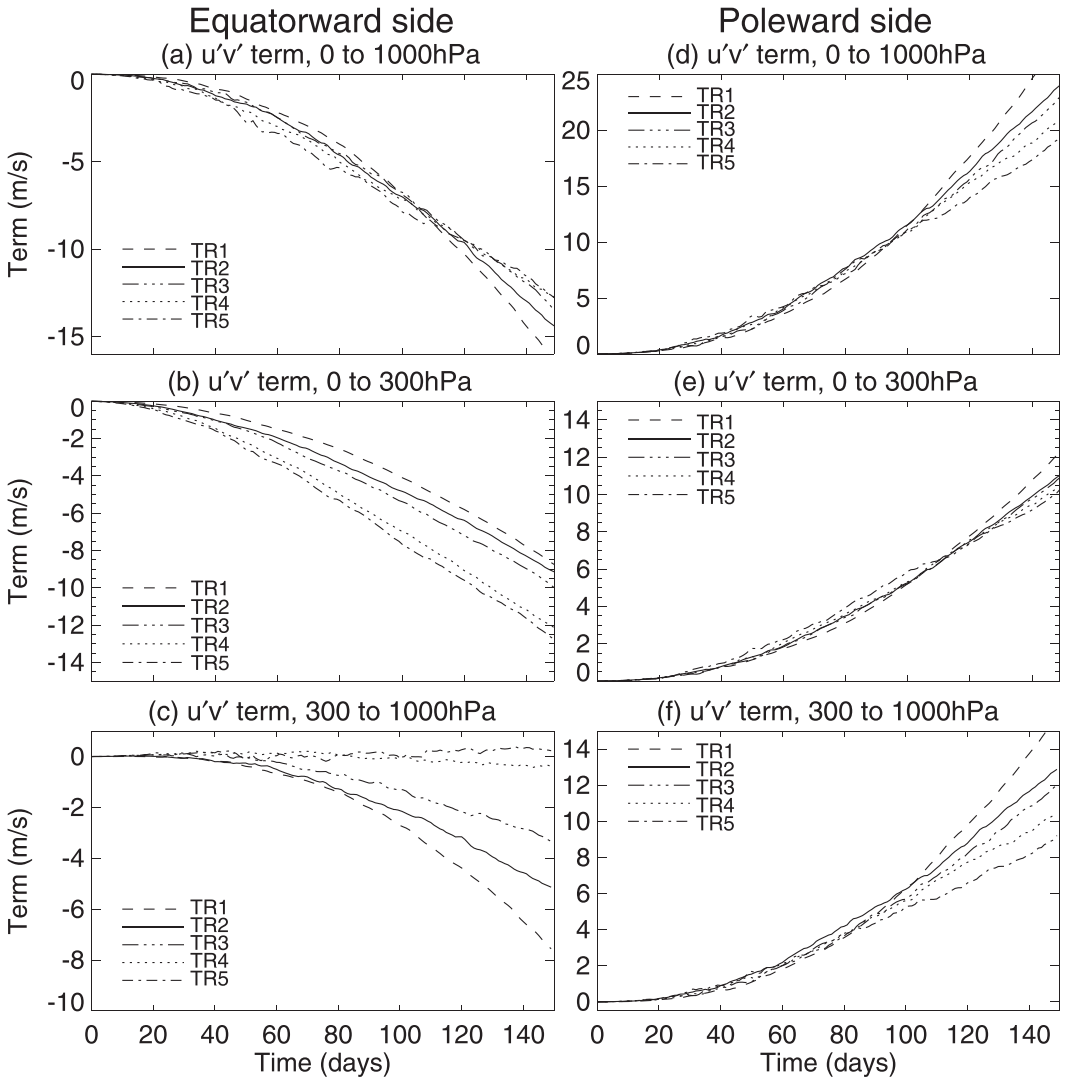

FIG. 8. The vertically averaged eddy momentum flux convergence term in Eq. (4) that contributes to the zonal wind anomalies for the (a)–(c) equatorward and (d)–(f) poleward side of the jet. (a),(d) Vertically averaged from the model lid to the surface; (b),(e) and (c),(f) the contributions from 0 to 300 hPa and 300 hPa to the surface, respectively.

the difference in this momentum flux anomaly between the tropospheres, as the wind anomalies and their meridional shears are very similar between the different jets.

The baroclinic component of the eddy feedback involves a shift in eddy source latitude associated with the decrease in baroclinicity on the equatorward side of the jet and increase on the poleward side. It is possible that there is a difference in the baroclinicity of the wind responses. Eddies grow in the region of high baroclinicity associated with the jet and, in their nonlinear phase, propagate mainly equatorward, resulting in a poleward momentum flux toward their latitude of origin (Fig. 1). This accelerates the zonal wind and, together with the action of surface friction, enhances baroclinicity in the eddy source region, providing a positive feedback (Robinson 2000; Chen and Plumb 2009; Kidston et al. 2010). A stronger baroclinic feedback of the eddies onto the mean flow would therefore require a larger increase in upward E-P flux in the region of zonal wind increase and a larger decrease in upward E-P flux in the region of zonal wind decrease.

Figure 9 examines the vertical E-P flux anomalies for days 40–70. There is very little difference in the magnitude of the upward E-P flux anomaly on the poleward side of the jet. Moreover, the decrease on the equatorward side of the jet is stronger and broader for higher-latitude jets. There is no indication that a difference in the anomalous eddy growth associated with the jet shift

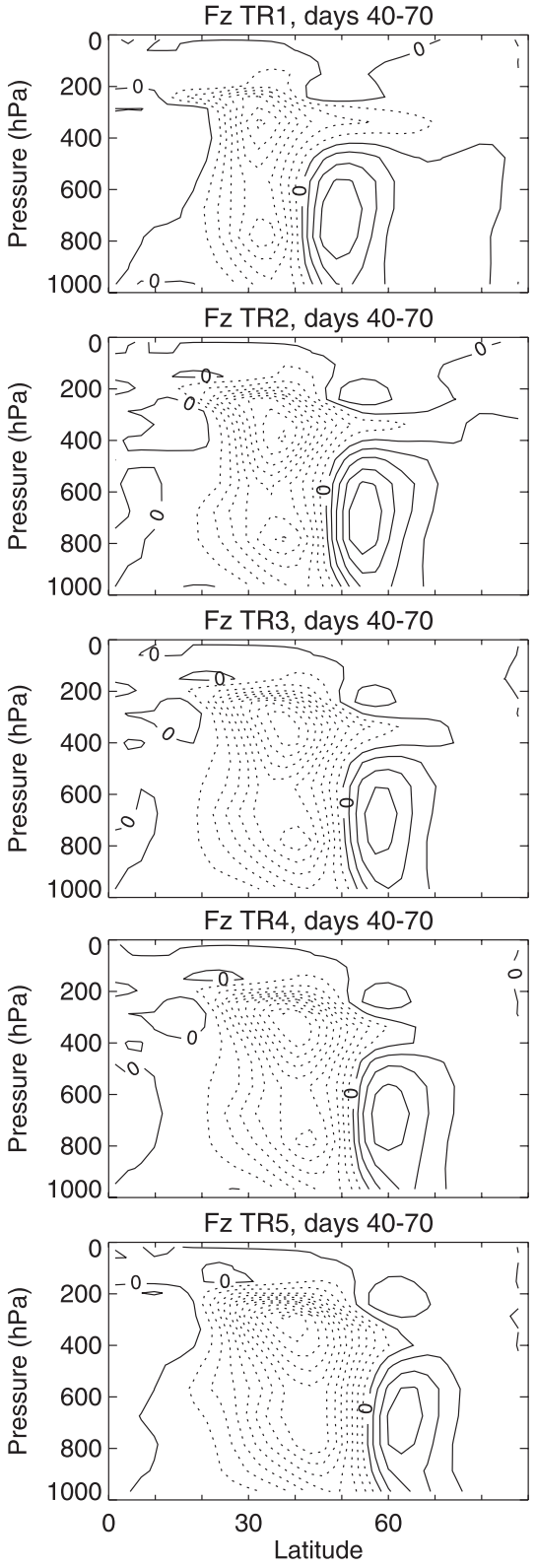

FIG. 9. Anomaly in vertical E-P flux for each troposphere averaged over days 40–70. Contour intervals are 10^5 Pa m^2 s^{-2} and solid and dotted contours represent positive and negative values, respectively.

is responsible for the enhanced feedback in TR1 compared to TR5. Rather, it must be some aspect of the eddy propagation that results in a stronger increase in eddy momentum flux divergence on the equatorward side of the jet for lower-latitude jets. To examine this further the eddy flux cospectra are next analyzed.

Column 1 of Fig. 10 shows the control run $\overline{u'v'}$ cospectra at 400 hPa for each troposphere. 400 hPa is below the subtropical reduction in $\overline{u'v'}$, so it allows the tropospheric feedback to be analyzed in isolation from the initial direct response. For all phase speeds, the maximum flux occurs slightly poleward of the critical line, as expected from critical layer control of eddy fluxes (Randel and Held 1991). Furthermore, the higher-latitude jets, which are also stronger, have a much greater range of phase speeds and much stronger eddy fluxes.

Columns 2 and 3 of Fig. 10 examine the anomalies in $\overline{u'v'}$ and $\overline{u'v'}$ convergence in response to the E5 heating calculated over the first 80 days of the spinup (with tapering by a cosine function over the first and last 8 days). This is the period before the wind anomalies become significantly different between the tropospheres but when there is already a noticeable difference in the tropospheric eddy momentum flux feedback on the equatorward side of the jet. The main component of the feedback in the early stage of the spinup is the altered meridional wind shear acting to enhance the equatorward refraction of the eddies. The $\overline{u'v'}$ anomalies are consistent with this. There is an enhanced poleward flux of momentum at all phase speeds resulting in enhanced momentum flux divergence just poleward of the low-latitude critical line.

Column 4 of Fig. 10 shows the wind anomaly averaged over days 0–80 (dashed) and the eddy momentum flux convergence anomaly, both output from the model (solid) and calculated from the cospectra (dotted). The latter two agree very well and any differences are most likely associated with the lowest phase speeds not being resolved by the cospectrum analysis. On the poleward side of the jet there is very little difference between the tropospheres. Each shows an increase in $\overline{u}$ of comparable magnitude associated with an enhanced $\overline{u'v'}$ convergence also of comparable magnitude. On the equatorward side of the jet the zonal wind decrease is also of comparable magnitude between the tropospheres, but it is associated with enhanced momentum flux divergence that does differ significantly (as was evident in Figs. 7 and 8). In each of the tropospheres the momentum flux divergence anomaly is displaced equatorward of the easterly wind anomaly. However, for the lower-latitude jets the displacement is smaller, giving more overlap with the wind anomaly, and the

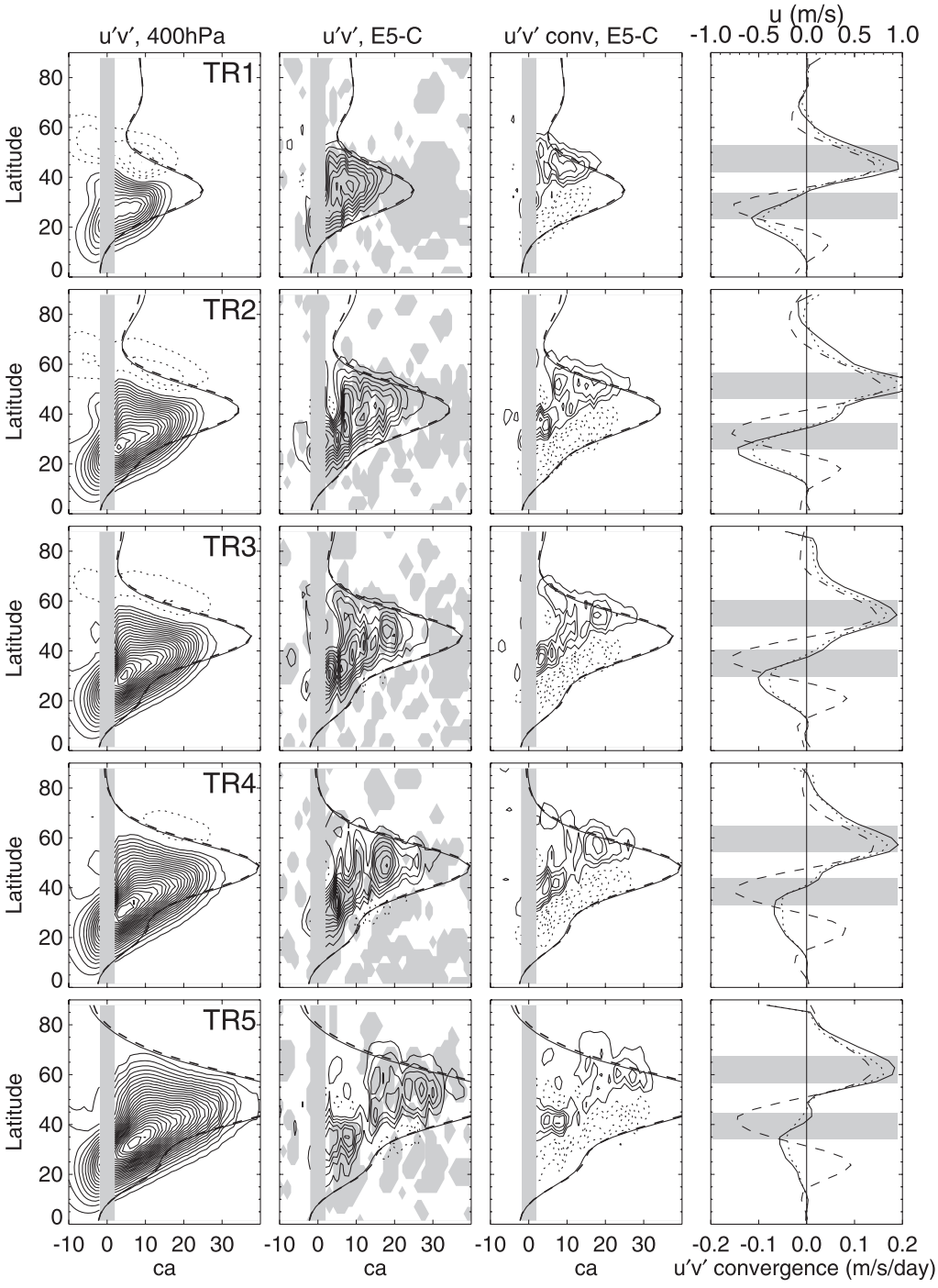

FIG. 10. Cospectra at 400 hPa. (column 1) Control run horizontal eddy momentum flux. Other columns show anomalies calculated from days 0–80 of the spinup. (column 2) Horizontal eddy momentum flux anomaly (gray regions are statistically different from zero at the 95% confidence level via a *t* test). Note that significance occurs in some regions of negligible flux anomaly because the variability in those regions is extremely small. These should be ignored. (column 3) Horizontal eddy momentum flux convergence anomaly. (column 4) Anomalies in zonal wind (dashed), horizontal eddy momentum flux convergence (solid), and horizontal eddy momentum flux convergence calculated from the cospectra (dotted). Contour intervals are (column 1) $0.1\ \mathrm{m^2\,s^{-2}}\ \Delta c_A^{-1}$, (column 2) $0.02\ \mathrm{m^2\,s^{-2}}\ \Delta c_A^{-1}$, and (column 3) $2 \times 10^{-3}\ \mathrm{m\,s^1\,day^{-1}}\ \Delta c_A^{-1}$, where Δc_A is $1\ \mathrm{m\,s^{-1}}$. In columns 1–3, the solid line shows the position of the control run critical line ($\overline{u}/\cos\phi$) and the dashed line shows the position of the critical line for the average of days 0–80. These are virtually identical. The 10° latitude bands in the region of maximum zonal wind decrease and increase are shaded gray in column 4.

momentum flux divergence anomaly is stronger and sharper. Both these effects result in a stronger eddy feedback for the lower-latitude jets.

This can be explained by the cospectra of momentum flux and its divergence in Fig. 10 (columns 2 and 3, respectively). Each phase speed in each troposphere shows a very similar response, consisting of a dipole with enhanced divergence just poleward of the critical line and enhanced convergence at higher latitudes, as expected from enhanced equatorward propagation of eddies that break around the low-latitude critical line. The momentum flux feedback for lower phase speed eddies occurs consistently close to the subtropical shoulder of the zonal wind profile for all the jets, just poleward of the low-latitude critical line for those phase speeds. Figure 2b shows that the subtropical zonal wind profile is relatively similar for each of the tropospheres while the midlatitude jet becomes increasingly separated from the subtropical westerlies going from TR1 to TR5. The higher-latitude jets therefore have a greater separation between the low and high phase speed critical lines. As a result, the low phase speed eddies fail to feed back positively onto the equatorward part of the zonal wind dipole, which is always located close to the midlatitude jet. In fact, the momentum flux forcing by low phase speed eddies becomes more separated from and begins to oppose that of high phase speed eddies for the more poleward jets, weakening their positive feedback. Figure 10 shows that, for TR4 and TR5, this cancellation occurs precisely at the latitude of the easterly wind anomaly on the equatorward flank of the jet, with the low phase speeds feeding back negatively there. The key reason for the larger separation of the high and low phase speed momentum flux forcings for higher-latitude jets is the larger separation of their low-latitude critical lines.

There is little difference between the magnitudes of the $\overline{u'v'}$ convergence anomalies on the poleward side of each jet. This is because low and high phase speed anomalies in the high-latitude jets only have different signed anomalies on the equatorward side. In TR5, on the poleward side of the jet, the convergence due to angular phase speeds of $10-30$ m s^{-1} acts in a similar manner to that due to angular phase speeds of $10-20$ m s^{-1} in TR1 and a similar magnitude of convergence results.

6. Discussion and conclusions

A reason has been proposed for the difference in the magnitude of the poleward shift of the jet in response to heating of the equatorial stratosphere, based on examination of the spinup evolution of five different jet structures. It is found that the main difference in response between the different jet structures lies in the strength of the eddy feedback onto the decreased zonal wind on the equatorward side of the jet.

In the early feedback stages of the spinup, the different jet structures differ in the magnitudes of the $\overline{u'v'}$ divergence on the equatorward side of the jet associated with the feedback processes. The $\overline{u'v'}$ divergence anomaly is narrower and stronger and projects more strongly onto the zonal wind anomalies for low-latitude jets compared to high-latitude jets. Thus, the lower-latitude jets have a stronger feedback between the eddies and the mean flow, despite having an initially weaker response (due to their weaker climatological fluxes). This is the primary reason for the difference in response between the different jets. Once this effect starts to produce a larger zonal wind anomaly for the lower-latitude jets, both the refraction feedback (equatorward propagation across the jet) and the baroclinic feedback (a poleward shift of the baroclinicity) become stronger, allowing the annular mode–like response to heating to grow larger for the lower-latitude jets.

The key to the difference in the strength of the feedback is a difference in the coherence of the behavior across the spectrum of eddy phase speeds. The higher-latitude jets used here exhibit a much wider range of phase speeds and a much wider latitudinal range of critical latitudes. As a result, different phase speed eddies do not act together to provide a positive feedback. In fact, the low phase speed eddies oppose the effect of the high phase speeds, reducing the deceleration on the equatorward side of the jet. This weakens the feedback between the tropospheric eddy momentum flux and the mean flow anomalies. The reduced correlation between the spatial patterns of $\overline{u'v'}$ convergence and $\overline{u}$ anomalies shown in Fig. 4 is a consequence of this. The increase in $\overline{u'v'}$ divergence on the equatorward side of the jet is broader and weaker for the higher-latitude jets and projects less well onto the zonal wind reduction on the equatorward side of the midlatitude jet.

The mechanism for a dependence of the response magnitude on climatological jet latitude has been proposed here for a particular forcing case. However, it may be relevant more generally, for example to explain the similar dependence found by Son et al. (2010) for polar stratospheric cooling associated with stratospheric ozone depletion and by Kidston and Gerber (2010) for anticipated climate change over the twenty-first century, since the difference between the jet structures lies in the strength of the tropospheric feedback. Such feedbacks should occur in response to any forcing that produces an annular mode–like zonal wind anomaly.

The fluctuation–dissipation theorem (Leith 1975) predicts that two dominant factors lead to a difference in the magnitude of an annular mode–like response to

a forcing for different jet structures: 1) the projection of the forcing onto the annular mode and 2) the time scale of natural annular mode variability, which depends on the strength of the feedback between the eddies and the mean flow. In the experiments reported here, it is the feedbacks that control the response magnitude. However, for other forcings, particularly those restricted to high latitudes, the projection onto the annular mode may be significantly reduced in the case of lower-latitude jets, counteracting the tendency for those jets to exhibit a stronger eddy feedback. In fact, SBHS10 found that an equatorward jet shift in response to polar stratospheric heating was also dependent on jet latitude, but that the sensitivity was less pronounced than for the poleward shift in response to equatorial heating.

Throughout this study, the discussion has been focused on an explanation of why there is a dependence on jet latitude of the response to forcings. However, the mechanism proposed actually suggests that the latitudinal range of critical latitudes on the equatorward side of the jet is key in determining the feedback strength. By construction each of these zonal wind structures has relatively similar subtropical westerly winds (Fig. 2b), so when the eddy-driven jet is at a higher latitude, the overall region of westerly winds is wider and a wider latitudinal range of critical latitudes exists on the equatorward side of the jet. This would also be true of the real atmosphere in seasons when the subtropical jet is present. Note that the subtropical zonal winds in TR1 are slightly farther poleward than those of all the other jets, narrowing the region of westerlies and enhancing the feedback even further for that troposphere.

The lower-latitude jets studied here are also weaker. If the lower-latitude jet was stronger, or the higher-latitude jet was weaker, then the difference in eddy feedback would be altered due to the greater or smaller range of phase speeds present. Based on the hypothesis in this study alone, one might expect that the stronger and narrower the jet, the stronger the eddy feedback and the larger the response. However, there is evidence from other studies that when the midlatitude jet becomes merged with the subtropical jet, such that there is a single strong jet, the strength of the eddy–mean flow feedbacks actually decrease (Eichelberger and Hartmann 2007; Barnes and Hartmann 2011). Eichelberger and Hartmann (2007) suggest that this is because a strong jet acts as a waveguide that inhibits the meridional propagation of waves away from their source latitude, resulting in a weakened eddy–mean flow feedback. Therefore, there may be other regimes to consider and it is possible that, within these, a strong, lower-latitude jet might exhibit a weaker response, but this remains to be tested.

Another mechanism that has been proposed for producing a poleward shift of the midlatitude jets in response to a forcing is through a change in the eddy phase speed. Chen et al. (2007) demonstrated that, in response to a reduction in surface friction in an sGCM, the phase speed of the dominant eddies increases. The relevant critical latitudes are therefore farther poleward so that a poleward shift of the horizontal eddy momentum flux results. While this is rather different from the case of stratospheric heating, as the zonal wind is initially altered at low levels, it has been proposed that altered vertical wind shear around the tropopause in response to stratospheric temperature perturbations could also act to increase the eddy phase speed and cause a shift in the jet (Chen and Held 2007), but this remains under debate (e.g., McLandress et al. 2010).

Eddy flux cospectra allow us to examine this for the case of E5 heating, which induces an increase in lower-stratospheric zonal wind at mid- to high latitudes (See Fig. 1 of SBH09). By the Chen et al. (2007) hypothesis, this could induce a change in the phase speed to produce the initial response. Figures 11a and 11b show, for the case of TR3, the control climatology and the anomaly for the average over days 0–50 of the spinup in the $\overline{u'v'}$ cospectra at 150 hPa (i.e., the level at which the initial decrease in $\overline{u'v'}$ occurs). The dominant component of the initial response is a reduction of the climatological $\overline{u'v'}$ on the equatorward side of the jet at all phase speeds rather than an increase in the momentum flux at high phase speeds at the expense of low phase speeds. The increase in $\overline{u'v'}$ on the poleward side of the jet is a signature of the start of the positive feedback associated with the equatorward refraction. Furthermore, Figs. 11c and 11d show the control and early spinup anomaly of the heat flux $\overline{v'T'}$ at 784 hPa to examine sources of anomalous eddy activity. There is a poleward shift rather than a clear dipole in phase speed, as found in Fig. 7 of Chen et al. (2007). The initial reduction in climatological momentum flux around the tropopause that triggers the tropospheric response does not appear to be related to anomalies in the eddy source (neither phase speed nor some other aspect of eddy generation). It remains to be seen whether other forcings such as ozone depletion, which may have a greater effect on the jet speed in the upper troposphere, act through this phase speed mechanism. However, these results do show that a change in lower-stratospheric temperature can trigger a change in the jet position through the influence of altered static stability around the tropopause on eddy propagation, rather than through changes occurring at the eddy source. Such an effect may also be important for the response to ozone depletion.

It remains to be confirmed whether the results of this simplified GCM study are relevant for more realistic

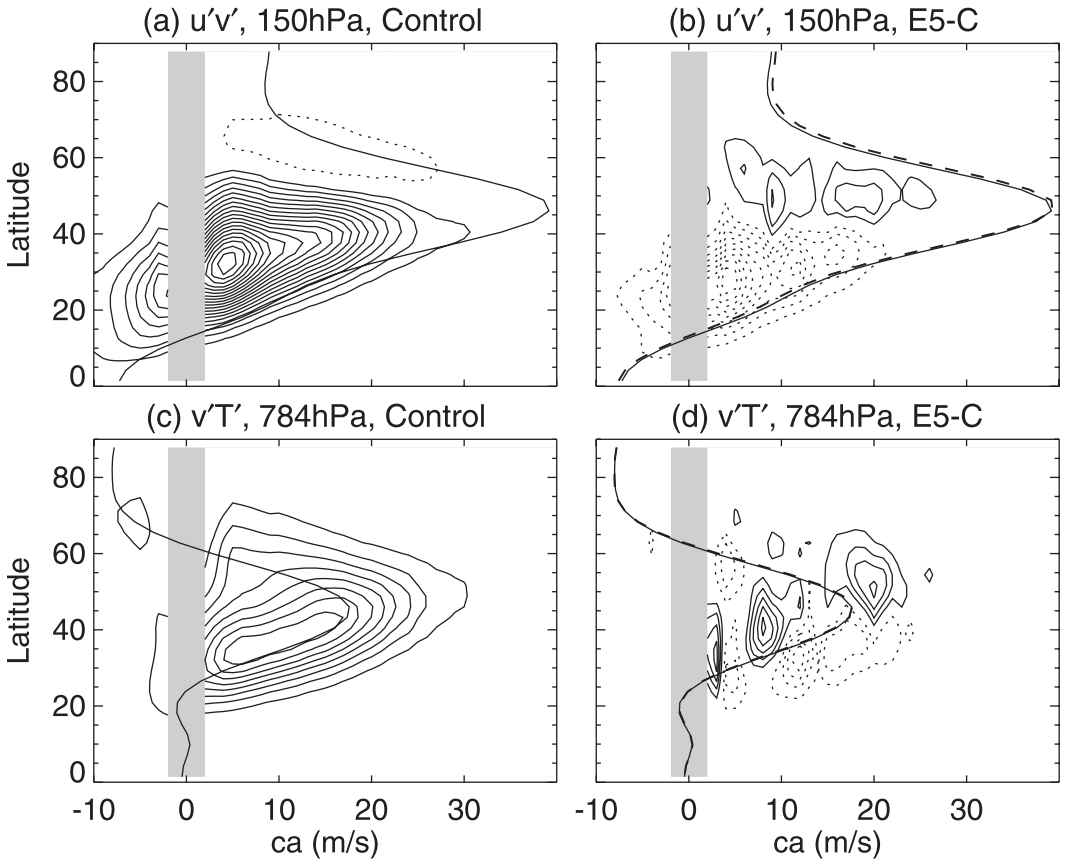

FIG. 11. Cospectra of the (a) TR3 control run $\overline{u'v'}$ at 150 hPa (contour interval = 0.1 m^2 s^{-2} Δc_A^{-1}), (b) TR3 $\overline{u'v'}$ E5 anomaly at 150 hPa calculated from days 0 to 50 of the spinup (contour interval = 0.02 m^2 s^{-2} Δc_A^{-1}), (c) TR3 control run $\overline{v'T'}$ at 784 hPa (contour interval = 0.1 K m s^{-1} Δc_A^{-1}), and (d) TR3 $\overline{v'T'}$ E5 anomaly at 784 hPa calculated from days 0 to 50 of the spinup (contour interval = 0.005 K m s^{-1} Δc_A^{-1}) where $\Delta c_A = 1$ m s^{-1}. The solid line on each plot shows the control run critical line at that level and the dashed line on the anomaly plots shows the E5 critical line averaged over days 0–50 of the spinup.

situations. In simplified GCM configurations such as that studied here, there are multiple regimes of zonal wind variability (Son et al. 2008a; Sparrow et al. 2009; Chan and Plumb 2009), in many cases with unrealistically long annular mode time scales. This means that the range of time scales between these different jet structures is extremely large (SBHS10) (e.g., TR1 has a mean time scale of around 90 days whereas TR5 has a mean time scale of around 30 days). Nevertheless, none of these jet structures exhibits a bimodal distribution in jet latitude as has been found to give rise to unrealistically long time scales in other sGCM studies (Chan and Plumb 2009). There are likely to be certain processes missing in sGCMs that are important for the real atmosphere. However, given that critical layer control of eddy fluxes occurs in the real atmosphere, it is reasonable to expect that the proposed hypothesis is relevant for more realistic configurations.

A mechanism has been identified that accounts for the dependence on jet latitude of the magnitude of the poleward shift of the jet in response to a forcing. In the jet configurations considered here the subtropical zonal wind structure is rather similar for each case but the latitude and strength of the eddy-driven jet vary. The result is that, in the mid- to upper troposphere, the higher-latitude jets have a wider latitudinal range of critical line locations on the equatorward side of the jet. This results in a lack of coherence in the momentum flux across the spectrum of eddy phase speeds, leading to a weaker eddy feedback. In general this effect may be influenced by a number of factors that affect the latitudinal range of critical latitudes, including the range of phase speeds present, variations in the subtropical zonal wind profile, and the possible presence of turning latitudes on either side of the jet. This raises the possibility of alternative regimes. The extent to which the phase speed coherence mechanism identified here will govern the magnitude of response in such situations remains to be investigated.

Acknowledgments. Simpson is very grateful to Charles McLandress for useful discussions as well as to Martin Keller and Gang Chen for advice on cospectra calculations. We are also grateful to Elizabeth Barnes and an anonymous reviewer for their helpful comments on this manuscript. This work was partly funded by the Natural Sciences and Engineering Research Council of Canada and partly by a UK Natural Environment Research Council PhD studentship.

REFERENCES

Barnes, E. A., and D. L. Hartmann, 2011: Rossby wave scales, propagation, and the variability of the eddy-driven jets. *J. Atmos. Sci.,* **68,** 2893–2908.

——, ——, D. M. W. Frierson, and J. Kidston, 2010: Effect of latitude on the persistence of eddy-driven jets. *Geophys. Res. Lett.,* **37,** L11804, doi:10.1029/2010GL043199.

Chan, C. J., and R. A. Plumb, 2009: The response to stratospheric forcing and its dependence on the state of the troposphere. *J. Atmos. Sci.,* **66,** 2107–2115.

Chen, G., and I. M. Held, 2007: Phase speed spectra and the recent poleward shift of Southern Hemisphere surface westerlies. *Geophys. Res. Lett.,* **34,** L21805, doi:10.1029/2007GL031200.

——, and R. A. Plumb, 2009: Quantifying the eddy feedback and the persistence of the zonal index in an idealized atmospheric model. *J. Atmos. Sci.,* **66,** 3707–3720.

——, I. M. Held, and W. M. Robinson, 2007: Sensitivity of the latitude of the surface westerlies to surface friction. *J. Atmos. Sci.,* **64,** 2899–2915.

Eichelberger, S. J., and D. L. Hartmann, 2007: Zonal jet structure and the leading mode of variability. *J. Climate,* **20,** 5149–5163.

Fyfe, J. C., and O. A. Saenko, 2006: Simulated changes in the extratropical Southern Hemisphere winds and currents. *Geophys. Res. Lett.,* **33,** L06701, doi:10.1029/2005GL025332.

Gerber, E. P., and G. K. Vallis, 2007: Eddy–zonal flow interactions and the persistence of the zonal index. *J. Atmos. Sci.,* **64,** 3296–3311.

——, S. Voronin, and L. M. Polvani, 2008: Testing the annular mode autocorrelation time scale in simple atmospheric general circulation models. *Mon. Wea. Rev.,* **136,** 1523–1536.

Haigh, J. D., M. Blackburn, and R. Day, 2005: The response of tropospheric circulation to perturbations in lower-stratospheric temperature. *J. Climate,* **18,** 3672–3685.

Hayashi, Y., 1971: A generalized method of resolving disturbances into progressive and retrogressive waves by space Fourier and time cross-spectral analyses. *J. Meteor. Soc. Japan,* **49,** 125–128.

Held, I. M., and M. J. Suarez, 1994: A proposal for the intercomparison of the dynamical cores of atmospheric general circulation models. *Bull. Amer. Meteor. Soc.,* **75,** 1825–1830.

Hoskins, B. J., and J. Simmons, 1975: A multi-layer spectral model and the semi-implicit method. *Quart. J. Roy. Meteor. Soc.,* **101,** 637–655.

Karoly, D. J., and B. J. Hoskins, 1982: Three-dimensional propagation of planetary waves. *J. Meteor. Soc. Japan,* **60,** 109–123.

Kidston, J., and E. P. Gerber, 2010: Intermodel variability of the poleward shift of the austral jet stream in the CMIP3 integrations linked to biases in 20th century climatology. *Geophys. Res. Lett.,* **37,** L09708, doi:10.1029/2010GL042873.

——, D. M. W. Frierson, J. A. Renwick, and G. J. Vallis, 2010: Observations, simulations, and dynamics of jet stream variability and annular modes. *J. Climate,* **23,** 6186–6199.

Kushner, P. J., 2010: Annular modes of the troposphere and stratosphere. *The Stratosphere: Dynamics, Transport, and Chemistry, Geophys. Monogr.,* Vol. 190, Amer. Geophys. Union, 59–91.

Lee, S., S.-W. Son, K. Grise, and S. B. Feldstein, 2007: A mechanism for the poleward propagation of zonal mean flow anomalies. *J. Atmos. Sci.,* **64,** 849–868.

Leith, C. E., 1975: Climate response and fluctuation dissipation. *J. Atmos. Sci.,* **32,** 2022–2026.

Lenton, A., F. Codron, L. Bopp, N. Metzl, P. Cadule, A. Tagliabue, and J. Le Sommer, 2009: Stratospheric ozone depletion reduces ocean carbon uptake and enhances ocean acidification. *Geophys. Res. Lett.,* **36,** L12606, doi:10.1029/2009GL038227.

Lorenz, D. J., and D. L. Hartmann, 2001: Eddy–zonal flow feedback in the Southern Hemisphere. *J. Atmos. Sci.,* **58,** 3312–3327.

——, and ——, 2003: Eddy–zonal flow feedback in the Northern Hemisphere winter. *J. Climate,* **16,** 1212–1227.

Matsuno, T., 1970: Vertical propagation of stationary planetary waves in the winter Northern Hemisphere. *J. Atmos. Sci.,* **27,** 871–883.

McLandress, C., T. G. Shepherd, J. F. Scinocca, D. A. Plummer, M. Sigmond, A. I. Jonsson, and M. C. Reader, 2010: Separating the dynamical effects of climate change and ozone depletion. Part II: Southern Hemisphere troposphere. *J. Climate,* **24,** 1850–1868.

Miller, R. L., G. A. Schmidt, and D. T. Shindell, 2006: Forced annular variations in the 20th century Intergovernmental Panel on Climate Change Fourth Assessment Report models. *J. Geophys. Res.,* **111,** D18101, doi:10.1029/2005JD006323.

Randel, W. J., and I. M. Held, 1991: Phase speed spectra of transient eddy fluxes and critical layer absorption. *J. Atmos. Sci.,* **48,** 688–697.

Robinson, W. A., 2000: A baroclinic mechanism for the eddy feedback on the zonal index. *J. Atmos. Sci.,* **57,** 415–422.

Seager, R., N. Harnick, Y. Kushnir, W. Robinson, and J. Miller, 2003: Mechanisms of hemispherically symmetric climate variability. *J. Climate,* **16,** 2960–2978.

Sigmond, M., and J. C. Fyfe, 2010: Has the ozone hole contributed to increased Antarctic sea ice extent? *Geophys. Res. Lett.,* **37,** L18502, doi:10.1029/2010GL044301.

Simmons, A. J., and D. M. Burridge, 1981: An energy and angular-momentum conserving vertical finite-difference scheme and hybrid vertical coordinates. *Mon. Wea. Rev.,* **109,** 758–766.

Simpson, I. R., M. Blackburn, and J. D. Haigh, 2009: The role of eddies in driving the tropospheric response to stratospheric heating perturbations. *J. Atmos. Sci.,* **66,** 1347–1365.

——, ——, ——, and S. N. Sparrow, 2010: The impact of the state of the troposphere on the response to stratospheric heating in a simplified GCM. *J. Climate,* **23,** 6166–6185.

Son, S.-W., and S. Lee, 2005: The response of westerly jets to thermal driving in a primitive equation model. *J. Atmos. Sci.,* **62,** 3741–3757.

——, and Coauthors, 2008a: The impact of stratospheric ozone recovery on the Southern Hemisphere westerly jet. *Science,* **320,** 1486–1489, doi:10.1126/science.1155939.

——, S. Lee, S. B. Feldstein, and J. E. Ten Hoeve, 2008b: Time scale and feedback of zonal-mean-flow variability. *J. Atmos. Sci.,* **65,** 935–952.

——, and Coauthors, 2010: Impact of stratospheric ozone on the Southern Hemisphere circulation changes: A multimodel assessment. *J. Geophys. Res.,* **115,** D00M07, doi:10.1029/2010JD014271.

SPARC CCMVal, 2010: SPARC report on the evaluation of chemistry–climate models. V. Eyring, T. G. Shepherd, and D. W. Waugh, Eds., SPARC Rep. 5, WCRP-132, WMO/TD–1526. [Available online at http://www.atmosp.physics.utoronto.ca/SPARC/ccmval_final/index.php.]

Sparrow, S., M. Blackburn, and J. D. Haigh, 2009: Annular variability and eddy–zonal flow interactions in a simplified atmospheric GCM. Part I: Characterization of high- and low-frequency behavior. *J. Atmos. Sci.,* **66,** 3075–3094.

Swart, N. C., and J. C. Fyfe, 2011: Ocean carbon uptake and storage influenced by wind bias in global climate models. *Nat. Climate Change,* **2,** 47–52.

Thompson, D. W. J., and J. M. Wallace, 2000: Annular modes in the extratropical circulation. Part I: Month-to-month variability. *J. Climate,* **13,** 1000–1016.

——, and S. Solomon, 2002: Interpretation of recent Southern Hemisphere climate change. *Science,* **296,** 895–899, doi:10.1126/science.1069270.

Thorncroft, C. D., B. J. Hoskins, and M. E. McIntyre, 1993: Two paradigms of baroclinic-wave life-cycle behaviour. *Quart. J. Roy. Meteor. Soc.,* **119,** 17–55.

Zickfeld, K., J. C. Fyfe, O. A. Saenko, M. Eby, and A. J. Weaver, 2007: Response of the global carbon cycle to human-induced changes in Southern Hemisphere winds. *Geophys. Res. Lett.,* **34,** L12712, doi:10.1029/2006GL028797.